

Excitations and the tangent space of projected entangled-pair states

Laurens Vanderstraeten,¹ Frank Verstraete,^{1,2} and Jutho Haegeman¹

¹*Ghent University, Department of Physics and Astronomy, Krijgslaan 281-S9, B-9000 Gent, Belgium*

²*Vienna Center for Quantum Science, Universität Wien, Boltzmannngasse 5, A-1090 Wien, Austria*

(Dated: September 18, 2022)

We introduce a variational ansatz for elementary excitations of two-dimensional quantum spin systems, directly in the thermodynamic limit, based on the formalism of projected entangled-pair states (PEPS). Solving the corresponding variational problem requires the evaluation of momentum transformed two-point and three-point correlation functions on a PEPS background, which we can compute efficiently by introducing a variation of the corner transfer matrix. Our approach can be readily extended to topologically non-trivial excitations (anyons) and is illustrated for the elementary excitations in the Affleck-Lieb-Kennedy-Tasaki model on the square lattice and a perturbed version of Kitaev's toric code. These developments give direct access to the low-energy sector of strongly correlated two-dimensional quantum systems and allow for the formulation of improved optimization algorithms for determining a variational PEPS ground state approximation.

In the last decades low-dimensional quantum systems have been at the forefront of both theoretical and experimental physics. With the reduced dimensionality allowing for stronger quantum correlations, these systems show an extreme variety of exotic phenomena but are notoriously difficult to simulate [1].

In one dimension, the advent of the density matrix renormalization group (DMRG) [2] has provided an extremely reliable and efficient method for describing strongly-correlated quantum systems. A better understanding of this success was realized through the identification of the variational class over which DMRG optimizes as *matrix product states* (MPS) [3, 4]. More specifically, it was understood how the entanglement structure of MPS allows for a natural parametrization of the low-energy states of local one-dimensional quantum systems [5].

The MPS construction can be extended to higher dimensions, leading to the formulation of *projected entangled-pair states* (PEPS) [6, 7]. This class of states has shown to capture the low-energy physics of several interesting systems in two dimensions and is competing with more established methods in determining their ground-state properties [8, 9]. Yet, in contrast to the one-dimensional case, the PEPS simulation of two-dimensional systems is computationally challenging, thus making the development of new algorithms highly desirable.

This article opens up a new approach for simulating two-dimensional quantum systems with PEPS. Our approach is inspired by the recent development of so-called *post-MPS* methods [10] for capturing the dynamics of one-dimensional systems on top of an MPS ground state. The central idea of these methods is that the low-energy dynamics are not taking place within the MPS manifold itself but rather in its *tangent space*, an idea which has led to the formulation of algorithms for ground state optimization and real-time simulation [11], and a variational ansatz for capturing elementary excitations [12, 13] and the scattering thereof [14].

One central ingredient for translating these methods to the two-dimensional case is the computation of two-

and three-point functions with respect to a PEPS ground state. We introduce a variation of the *corner transfer matrix* [15–17] that renders this task efficient. In a next step, we write down the PEPS version of the Feynman-Bijl ansatz [18, 19] for variationally determining elementary excitation spectra, and show how to compute one-particle dispersion relations and spectral weights. We apply these methods to compute the excitation spectrum of the two-dimensional AKLT model and the filtered toric code.

PEPS and the corner transfer matrix. Consider a two-dimensional quantum lattice system in the thermodynamic limit. A translation-invariant PEPS [6] can be parametrized by a single five-legged tensor $A_{u,r,d,l}^s$ as

$$|\Psi(A)\rangle = \sum_{\{s\}=1}^d C_2(\{A^s\}) |\{s\}\rangle$$

where $C_2(\dots)$ denotes the contraction of an infinite two-dimensional network of A tensors. Pictorially we can write this down as

$$|\Psi(A)\rangle = \text{Diagram of a 2D lattice of red tensors } A \text{ with four virtual legs and one physical leg } s. \quad (1)$$

where we have represented the tensor A as

$$A_{u,l,d,r}^s = \text{Diagram of a red tensor with legs } u, l, d, r \text{ and } s.$$

The dimension of the four *virtual* legs (u, r, l, d) is called the bond dimension D of the PEPS and serves as a refinement parameter of the variational class, whereas the leg s has the local physical dimension d . In diagrams such as in Eq. (1) whenever two legs are connected the two corresponding indices are contracted (i.e. identified and summed over), such that $|\Psi(A)\rangle$ is obtained by contracting virtual legs of neighbouring tensors [20].

Computing the norm or a local expectation value of a PEPS involves the contraction of an infinite tensor network. Indeed, denoting the “double layer” tensor a as

$$a_{uu',rr',dd',ll'} = \sum_s A_{uldr}^s \otimes \bar{A}_{u'l'd'r'}^s = \text{Diagram of two red tensors } A \text{ and } \bar{A} \text{ with legs } u, u', r, r', d, d', l, l' \text{ and } s. = \text{Diagram of a square with legs } u, u', r, r'.$$

give rise to states with zero norm. Correspondingly, the *effective norm matrix* $\mathbf{N}_{\text{eff}}^{\kappa_x \kappa_y}$, defined as

$$\begin{aligned} \langle \Phi_{\kappa'_x \kappa'_y}(B') | \Phi_{\kappa_x \kappa_y}(B) \rangle \\ = 4\pi^2 \delta(\kappa_x - \kappa'_x) \delta(\kappa_y - \kappa'_y) \mathbf{B}' \mathbf{N}_{\text{eff}}^{\kappa_x \kappa_y} \mathbf{B}, \end{aligned}$$

will have a number of zero eigenvalues (\mathbf{B} is the vector containing all elements of the tensor B). In order for the variational subspace to be well-defined, we will always project out these null modes. In addition, since we want an excitation to be orthogonal to the ground state, we will also project out the component that is proportional to the ground state tensor A .

Once we have defined the variational subspace, we can minimize the energy in order to find the best approximation to the true excitation. Since the subspace is linear, this can be done by solving the Rayleigh-Ritz problem

$$\mathbf{H}_{\text{eff}}^{\kappa_x \kappa_y} \mathbf{B} = \omega \mathbf{N}_{\text{eff}}^{\kappa_x \kappa_y} \mathbf{B}$$

where the *effective Hamiltonian matrix* $\mathbf{H}_{\text{eff}}^{\kappa_x \kappa_y}$ is similarly defined as (E_0 is the ground-state energy)

$$\begin{aligned} \langle \Phi_{\kappa'_x \kappa'_y}(B') | \hat{H} - E_0 | \Phi_{\kappa_x \kappa_y}(B) \rangle \\ = 4\pi^2 \delta(\kappa_x - \kappa'_x) \delta(\kappa_y - \kappa'_y) \mathbf{B}' \mathbf{H}_{\text{eff}}^{\kappa_x \kappa_y} \mathbf{B}. \end{aligned}$$

The matrix elements of $\mathbf{N}_{\text{eff}}^{\kappa_x \kappa_y}$ and $\mathbf{H}_{\text{eff}}^{\kappa_x \kappa_y}$ contain two- and three-point functions that can be computed with a channel environment as in Eq. (4). The lowest eigenvalue ω corresponds to the lowest excitation energy at momentum (κ_x, κ_y) . By repeating this procedure for different momenta, we can obtain the dispersion relation for all one-particle excitations in the system. Moreover, with an expression for the wave functions, we can straightforwardly compute their spectral weights.

Application 1. First we study the two-dimensional Affleck-Lieb-Kennedy-Tasaki (AKLT) model [27] on the square lattice. The one-dimensional AKLT model was first introduced to establish the existence of a gap in a rotationally invariant spin-1 chain, in support of the Haldane conjecture [28]. The construction can be straightforwardly extended to two-dimensional systems, but the existence of a gap – although highly expected – can no longer be established rigorously. On the square lattice the AKLT state can be represented as a PEPS with bond dimension $D = 2$, and is the unique ground state of

$$H_{\text{AKLT}} = \frac{1}{28} \sum_{\langle ij \rangle} h_{ij} + \frac{7}{10} h_{ij}^2 + \frac{7}{45} h_{ij}^3 + \frac{1}{90} h_{ij}^4$$

with $h_{ij} = \vec{S}_i \cdot \vec{S}_j$ the spin-2 Heisenberg interaction.

In Refs. 19 and 29 it was argued that the correlations in the AKLT state can be expressed as thermal averages of a related classical model in the same number of dimensions, contrary what one expects for generic quantum ground states. The real-space correlations then decay according to the 2D Ornstein-Zernike form $s(\vec{n}) = \langle \Psi(A) | \hat{O}_{\vec{n}} \hat{O}_{\vec{0}} | \Psi(A) \rangle \propto e^{-|\vec{n}|/\xi} e^{i\vec{\kappa}^* \cdot \vec{n}} / \sqrt{n}$ ($n \gg 1$). In

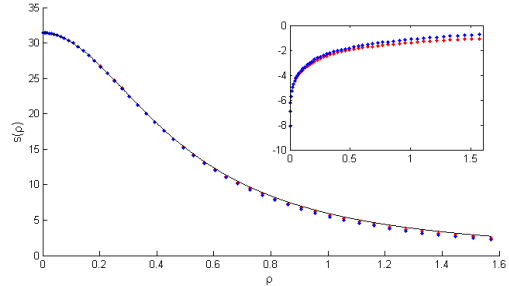


FIG. 1. The structure factor $s(\rho)$ where $\rho = ((\kappa_x - \pi)^2 + (\kappa_y - \pi)^2)^{1/2}$ for the two-dimensional AKLT model along the axes $\kappa_y = \pi$ (red) and $\kappa_x = \kappa_y$ (blue) compared to the form in Eq. (6). In the inset the (\log_{10}) of the deviations are plotted. The plot shows that the classical Ornstein-Zernike form is accurate for a large portion of the Brillouin zone and that the structure factor is nicely isotropic around $\vec{\kappa}^* = (\pi, \pi)$.

momentum space, the structure factor is thus given by

$$s(\vec{\kappa}) = \sum_{\vec{n}} e^{i\vec{\kappa} \cdot \vec{n}} s(\vec{n}) \propto \frac{1}{1 + \xi^2 |\vec{\kappa} - \vec{\kappa}^*|^2} \quad (6)$$

for momenta close to $\vec{\kappa}^*$ where $s(\vec{\kappa})$ reaches its maximum.

We can confirm this result with our methods. Firstly, we can calculate the correlation length by computing the gap of the linear transfer matrix \mathcal{T} using the methods of Ref. [24]. We obtain the value

$$\xi_{\text{AKLT}} = \frac{-1}{\log |\lambda_{\mathcal{T}}^{(2)}|} = 2.06491, \quad (7)$$

in reasonable agreement with the value of $\xi^{-1} \approx 0.52$ in Ref. 30. In Fig. 1 we compare the computation of the structure factor with our methods [Eq. (10)] with the form of Eq. (6) and observe very good agreement in a large portion of the Brillouin zone.

Going over to the actual excitations, we start with the single-mode approximation (SMA), which is known to reproduce the one-particle dispersion relation qualitatively in the one-dimensional case [19]. In the present context the SMA wave function is given by ($\alpha = x, y, z$)

$$|\Phi_{\kappa_x, \kappa_y}^\alpha \rangle_{\text{SMA}} = \sum_{m, n} e^{i(\kappa_x m + \kappa_y n)} \hat{S}_{(m, n)}^\alpha |\Psi_{\text{AKLT}}\rangle$$

and gives rise to the dispersion relation in Fig. 2. The spectrum consists of an elementary triplet with its minimum at $\kappa_{x, y} = \pi$ [23] and a gap $\Delta_{\text{SMA}} = 0.0199$.

In a next step we can determine the excitations variationally with the excitation ansatz [Eq. (5)]. At bond dimension $D = 2$ the number of variational parameters is too small to improve on the SMA result. In order to get a better estimate for the excitation energies, we enlarge the variational subspace by acting on more than one site – a procedure that is bound to converge exponentially fast to the correct excitation energy [13]. By introducing a B tensor on a block of two by two sites, we are able to estimate the gap at [31]

$$\Delta_{\text{var}} = 0.0147,$$

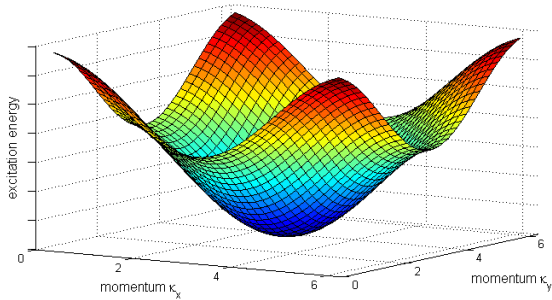


FIG. 2. Single mode approximation for the dispersion relation of the two-dimensional AKLT model on a square lattice. The minimum of the triplet dispersion relation is at momentum $\kappa_{x,y} = \pi$.

in excellent agreement with the value $2\Delta = 0.03$ in Ref. 32, obtained through a computation of the magnetization curve. In addition, we can compute the characteristic velocity through the second derivative of the dispersion relation in its minimum and we obtain $v_{\text{var}} = 0.04115$. By assuming an effective Lorentz invariance around the minimum, we can – via the Källén-Lehmann representation of the correlation functions $s(\vec{\kappa}) \propto (\Delta^2 + v^2|\vec{\kappa} - \vec{\kappa}^*|^2)^{-1/2}$ – estimate the correlation length variationally as

$$\xi_{\text{var}} = \sqrt{\frac{v_{\text{var}}^2}{2\Delta^2}} = 1.975$$

in reasonable agreement with the value in Eq. 7. Still better agreement should be possible by growing the block size in the ansatz, though this becomes computationally intractable; for block size 2×2 the number of variational parameters is already $\mathcal{O}(D^8 d^4)$.

Application 2. As a second example we study the anyonic excitations in the toric code [33], the easiest example of a model exhibiting topological order and anyonic excitations (fluxes and charges). At the toric code fixed point, the anyons have a flat dispersion relation since all Hamiltonian terms commute. In order to generate non-trivial dynamics we apply a local filtering to the system, generated by the filtering operator at site i

$$f_i = \exp\left(\frac{1}{4}(\beta_x \sigma_i^x + \beta_z \sigma_i^z)\right).$$

The Hamiltonian of the filtered toric code is given by

$$H_{\text{FTC}} = \sum_s \tilde{H}_s + \sum_p \tilde{H}_p$$

where the filtered star operators are given by

$$\tilde{H}_s = \left(\prod_{i \in s} f_i^{-1}\right) \left(1 - \prod_i \sigma_i^x\right) \left(\prod_{i \in s} f_i^{-1}\right)$$

and similar for the plaquette operator \tilde{H}_p with σ_i^z for $i \in p$. In first order, the filtering operation is equivalent to applying a magnetic field to the toric code. In fact,

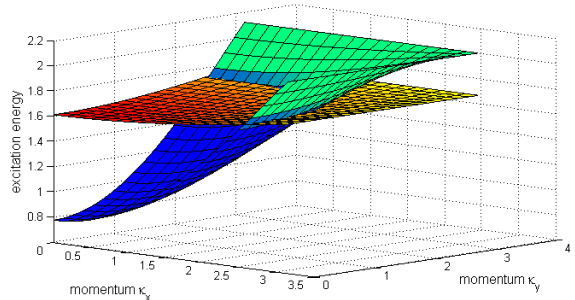


FIG. 3. The dispersion relation of the toric code in the flux (blue-green) and charge (red-yellow) sector for filtering parameters $\beta_x = 0.05$ and $\beta_z = 0.35$. For the former, we have used the topological ansatz with a string of σ^z operators at the virtual level, whereas the latter was obtained with an excitation that carries no string but transforms according to the odd representation of the virtual \mathbb{Z}_2 symmetry (note that we did not impose this symmetry on the B -tensor in Eq. (5) explicitly).

it has been shown in Refs. 24 and 34 that the phase diagram is qualitatively similar.

In a number of recent works it has been established that PEPS can provide a natural description of topological phases, where the topological order of the global state is reflected by a symmetry of the local PEPS tensor A on the virtual level [35, 36]. A variational ansatz for the complete set of elementary excitations in the different anyon sectors is obtained by attaching a half-infinite virtual matrix product operator string to the local B tensor in the excitation ansatz [Eq. (5)]. The topological sector is encoded in the type of string and the virtual symmetry representation of the local tensor. In the case of the toric code, the flux of the excitations is encoded in the presence or absence of a string of σ^z operators, whereas the charge is encoded in the symmetry representation of the B tensor [35]. These topological characteristics are unaltered by the filtering.

In Fig. 3 we have plotted the elementary excitation spectrum in both the charge and flux sector for a specific value of the filtering parameters. We can see that the filtering in one direction mostly affects one of the two excitations. This is reflected more clearly in Fig. 4, where we have plotted the gap in both sectors along the $\beta_x = 0$ axis. As explained in the caption, this figure essentially shows the condensation of flux excitations.

Conclusions. In this paper we have shown how to compute structure factors of a generic two-dimensional PEPS in the thermodynamic limit using the corner transfer matrix method. We have used this algorithm to determine the elementary excitations on top of a PEPS ground state variationally and applied these methods to the AKLT model and the filtered toric code. These two examples have an exact PEPS ground state, which simplifies the computation of the energy expectation values but disallowed us to systematically grow the bond dimension in order to improve on the variational excitations. Applying our methods to models with a variationally de-

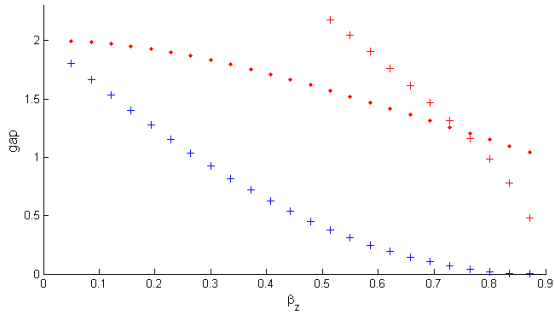


FIG. 4. The lowest-lying excitation energies in the charge and flux sector in function of β_z and with $\beta_x = 0$, for which the model can be shown to have a phase transition at $\beta_z = \log(\sqrt{2} + 1) \approx 0.88$ [37]. The color represents trivial (red) or non-trivial (blue) flux of the excitations, whereas the symbol represents even (+) or odd (-) charge number. We can observe that the gap in the flux sector closes, signalling the condensation of the flux excitations. Although our variational ansatz is not suited for describing multi-particle states, we can see the two-flux state (trivial sector and no charge) coming down in energy close to the phase transition. The charge excitation remains gapped.

terminated PEPS ground state will allow to compute excitation spectra of generic two-dimensional quantum systems [38].

In the one-dimensional case, the local description of excitations in the MPS framework led to the development of an effective particle picture of excitations on top of a strongly-correlated vacuum [14]. Our methods open up the route to a two-dimensional generalization of this particle description of the low-energy dynamics and, more specifically, to the formulation of the scattering problem for effective particles in two dimensions.

Finally, the methods we have presented enable the introduction of *post-PEPS* methods for variational optimization and real-time evolution. Indeed, with the channel structure of the effective environment we are able to compute both the gradient and the Hessian. These could be used in advanced variational algorithms. In contrast to other PEPS algorithms, these would take the globally optimal search direction into account and could therefore lead to more efficient optimization strategies [38].

The authors would like to thank Michaël Mariën for helpful discussions. Research supported by the Research Foundation Flanders (LV,JH), ARAG (LV) the Austrian FWF SFB grants FoQuS and ViCoM, and the European grants SIQS and QUTE (FV).

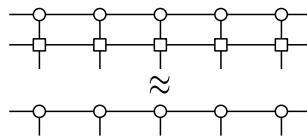
-
- [1] E. Fradkin, *Field Theories of Condensed Matter Physics*, 2nd ed. (Cambridge University Press, Cambridge, 2013).
[2] S. R. White, *Physical Review Letters* **69**, 2863 (1992).
[3] M. Fannes, B. Nachtergaele, and R. F. Werner, *Communications in Mathematical Physics* **144**, 443 (1992).
[4] S. Östlund and S. Rommer, *Physical Review Letters* **75**,

- 13 (1995); S. Rommer and S. Östlund, *Physical Review B* **55**, 2164 (1997).
[5] M. B. Hastings, *Journal of Statistical Mechanics: Theory and Experiment* **2007**, P08024 (2007); F. Verstraete and J. I. Cirac, *Physical Review B* **73**, 094423 (2006).
[6] F. Verstraete and J. I. Cirac, (2004), arXiv:0407066 [cond-mat]; F. Verstraete, M. Wolf, D. Pérez-García, and J. I. Cirac, *Physical Review Letters* **96**, 220601 (2006).
[7] F. Verstraete, V. Murg, and J. I. Cirac, *Advances in Physics* **57**, 143 (2008); R. Orús, *Annals of Physics* **349**, 117 (2014).
[8] J. Jordan, R. Orús, G. Vidal, F. Verstraete, and J. I. Cirac, *Physical Review Letters* **101**, 250602 (2008).
[9] V. Murg, F. Verstraete, and J. I. Cirac, *Physical Review A* **75**, 033605 (2007); S. Dusuel, M. Kamfor, R. Orús, K. P. Schmidt, and J. Vidal, *Physical Review Letters* **106**, 107203 (2011); P. Corboz, M. Lajkó, A. M. Läuchli, K. Penc, and F. Mila, *Physical Review X* **2**, 041013 (2012); D. Poilblanc, P. Corboz, N. Schuch, and J. I. Cirac, *Physical Review B* **89**, 241106 (2014); J. O. Iregui, P. Corboz, and M. Troyer, *Physical Review B* **90**, 195102 (2014); P. Corboz, T. M. Rice, and M. Troyer, *Physical Review Letters* **113**, 046402 (2014); P. Corboz and F. Mila, *Physical Review Letters* **112**, 147203 (2014).
[10] J. Haegeman, T. J. Osborne, and F. Verstraete, *Physical Review B* **88**, 075133 (2013).
[11] J. Haegeman, J. I. Cirac, T. J. Osborne, I. Pižorn, H. Verschelde, and F. Verstraete, *Physical Review Letters* **107**, 070601 (2011); J. Haegeman, C. Lubich, I. Osleedets, B. Vandereycken, and F. Verstraete, (2014), arXiv:1408.5056.
[12] J. Haegeman, B. Pirvu, D. J. Weir, J. I. Cirac, T. J. Osborne, H. Verschelde, and F. Verstraete, *Physical Review B* **85**, 100408 (2012).
[13] J. Haegeman, S. Michalakis, B. Nachtergaele, T. J. Osborne, N. Schuch, and F. Verstraete, *Physical Review Letters* **111**, 080401 (2013).
[14] L. Vanderstraeten, J. Haegeman, T. J. Osborne, and F. Verstraete, *Physical Review Letters* **112**, 257202 (2014); L. Vanderstraeten, J. Haegeman, and F. Verstraete, (2015), arXiv:1506.01008.
[15] R. J. Baxter, *Journal of Mathematical Physics* **9**, 650 (1968); *Exactly Solved Models in Statistical Mechanics* (Academic Press, London, 1982).
[16] T. Nishino and K. Okunishi, *Journal of the Physical Society of Japan* **65**, 891 (1996); *Journal of the Physical Society of Japan* **66**, 3040 (1997); *Journal of the Physical Society of Japan* **67**, 1492 (1998).
[17] R. Orús and G. Vidal, *Physical Review B* **80**, 094403 (2009); R. Orús, *Physical Review B* **85**, 205117 (2012); P. Corboz, J. Jordan, and G. Vidal, *Physical Review B* **82**, 245119 (2010).
[18] R. P. Feynman, *Physical Review* **91**, 1301 (1953); R. P. Feynman and M. Cohen, *Physical Review* **102**, 1189 (1956); S. M. Girvin, A. MacDonald, and P. Platzman, *Physical Review Letters* **54**, 581 (1985); *Physical Review B* **33**, 2481 (1986).
[19] D. P. Arovass, A. Auerbach, and F. D. M. Haldane, *Physical Review Letters* **60**, 531 (1988).
[20] In this paper we restrict to the square lattice, but our framework can be readily extended to more general lattices.
[21] N. Schuch, M. Wolf, F. Verstraete, and J. I. Cirac, *Physical Review Letters* **98**, 140506 (2007).
[22] M. Lubasch, J. I. Cirac, and M.-C. Bañuls, *New Journal of Physics* **16**, 033014 (2014).

- [23] V. Zauner, D. Draxler, L. Vanderstraeten, M. Degroote, J. Haegeman, M. M. Rams, V. Stojevic, N. Schuch, and F. Verstraete, *New Journal of Physics* **17**, 053002 (2015).
- [24] J. Haegeman, V. Zauner, N. Schuch, and F. Verstraete, (2014), arXiv:1410.5443.
- [25] We refer to the Supplemental Material for additional details.
- [26] U. Schollwöck, *Annals of Physics* **326**, 96 (2011).
- [27] I. Affleck, T. Kennedy, E. H. Lieb, and H. Tasaki, *Physical Review Letters* **59**, 799 (1987); *Communications in Mathematical Physics* **115**, 477 (1988).
- [28] F. D. M. Haldane, *Physical Review Letters* **50**, 1153 (1983); *Physics Letters A* **93**, 464 (1983).
- [29] D. P. Arovas and S. M. Girvin, in *Recent Progress in Many-Body Theories*, edited by T. L. Ainsworth, C. E. Campbell, B. E. Clements, and E. Krotscheck (Springer US, Boston, MA, 1992).
- [30] Y. Hieida, K. Okunishi, and Y. Akutsu, *New Journal of Physics* **1**, 7 (1999).
- [31] This value is quite small because of the prefactor of $\frac{1}{28}$ making the AKLT Hamiltonian a projector.
- [32] A. Garcia-Saez, V. Murg, and T.-C. Wei, *Physical Review B* **88**, 245118 (2013).
- [33] A. Kitaev, *Annals of Physics* **303**, 2 (2003).
- [34] J. Haegeman, K. Van Acoleyen, N. Schuch, J. I. Cirac, and F. Verstraete, *Physical Review X* **5**, 011024 (2015).
- [35] N. Schuch, I. Cirac, and D. Pérez-García, *Annals of Physics* **325**, 2153 (2010).
- [36] M. B. Şahinoğlu, D. Williamson, N. Bultinck, M. Mariën, J. Haegeman, N. Schuch, and F. Verstraete, (2014), arXiv:1409.2150.
- [37] C. Castelnovo and C. Chamon, *Physical Review B* **77**, 054433 (2008).
- [38] L. Vanderstraeten et. al., in preparation.
- [39] I. P. McCulloch, (2008), arXiv:0804.2509.

SUPPLEMENTAL MATERIAL

Transfer matrix and fixed points. In the first part of this Supplemental Material we study the fixed points of the linear transfer matrix \mathcal{T} and corner transfer matrix \mathcal{C} . For a translation-invariant MPS to satisfy the fixed point equation of the linear transfer matrix \mathcal{T}

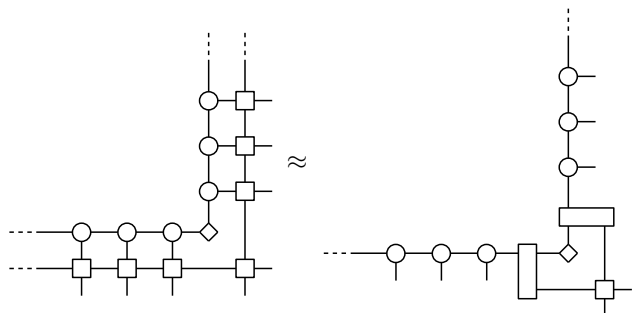


it is required that there exists a tensor (rectangle) such that

(8)

holds up to small truncation errors.

Let us now show that the “fixed point” of the corner transfer matrix \mathcal{C} should indeed be of the form that was given in Eq. (3). Note, firstly, that the corner transfer matrix introduces two new sites at every application (similar to infinite-size DMRG algorithms [2, 39]) and therefore does not have a fixed point in the strict sense. Nevertheless, repeated application of \mathcal{C} is likewise expected to result in a state with a converged (i.e. translation-invariant) structure, up to the corner itself. We therefore model the “fixed point” using the tensors of the fixed point of the linear transfer matrix and insert a new corner tensor. Applying the corner transfer matrix \mathcal{C} once and using the tensor from Eq. (8) gives rise to



which shows that the original MPS tensors are indeed obtained after application of \mathcal{C} , except on the two newly introduced sites. In principle, two new MPS tensors connected by a new corner matrix could appear. However, since the unique MPS tensor of the fixed point of \mathcal{T} seem to capture the correct structure on the further sites, and these two can be assumed to have originated from previous applications of \mathcal{C} , we can make the ansatz that these tensors should

also be put on the two new sites. With this ansatz, we obtain a linear fixed point equation for the corner matrix itself, which corresponds to a simple eigenvalue equation. With the corner matrix as only variational parameters in the fixed point equation for \mathcal{C} , we essentially have a linear subspace as ansatz and can therefore easily measure the error obtained by projecting onto this subspace.

Two-point functions. In the second part we show how to compute the overlap of two excitations of the form in Eq. (5). The computation of the momentum space correlation function (structure factor) [Eq. (6)] is a special case by replacing the tensor B with the application of an operator to a ground state A tensor.

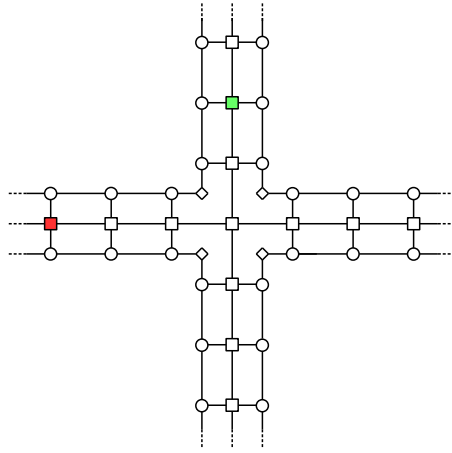
The overlap between two momentum superpositions of a local tensor yields the following double (infinite) sum

$$\langle \Phi_{\vec{\kappa}'}[B'] | \Phi_{\vec{\kappa}}[B] \rangle = \sum_{\vec{n}, \vec{n}'} e^{i(\vec{\kappa} \cdot \vec{n} - \vec{\kappa}' \cdot \vec{n}')} [B \text{ at site } \vec{n} \text{ and } B' \text{ at site } \vec{n}'].$$

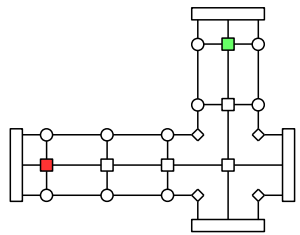
Because the ground state is translation invariant, we can simplify to a single sum as

$$\langle \Phi_{\vec{\kappa}'}[B'] | \Phi_{\vec{\kappa}}[B] \rangle = 4\pi^2 \delta^2(\vec{\kappa}' - \vec{\kappa}) \sum_{m, n'} e^{i\kappa_V m} e^{-i\kappa_H n'} [B \text{ at site } (m, 0) \text{ and } B' \text{ at site } (0, n')].$$

These terms are all two-point functions, which can be computed with our channel environment [Eq. (4)]. One term looks like



where the green (red) tensors indicate the locations of B and B' . In a first step we can contract the infinite channels by computing the fixed point of the “channel operators” and represent these as three-legged rectangles



The momentum superpositions can be worked out by inverting the relevant channel operator. For example, we can write one of the sums as

$$\sum_{m=1}^{\infty} e^{i\kappa_V m} [B \text{ at site } (m, 0) \text{ and } B' \text{ at site } (0, 0)]$$

$$= e^{i\kappa_V} \text{[diagram]} + e^{2i\kappa_V} \text{[diagram]} + e^{3i\kappa_V} \text{[diagram]} + \dots$$

$$= e^{+i\kappa_V} \text{ [Diagram: A tensor network with a red square in the center and a green square at the bottom, connected by vertical lines and diamond-shaped corner tensors.] }$$

where

$$\text{ [Diagram: A horizontal three-leg tensor with a central square and three legs.] } = \sum_{m=0}^{\infty} e^{i\kappa m} \left(\text{ [Diagram: A three-leg tensor with a central square and three legs, with a small square in the center.] } \right)^m = \left(1 - e^{i\kappa} \text{ [Diagram: A three-leg tensor with a central square and three legs, with a small square in the center.] } \right)^{-1}. \quad (9)$$

Applying this procedure to all geometric sums and keeping the local term amounts to

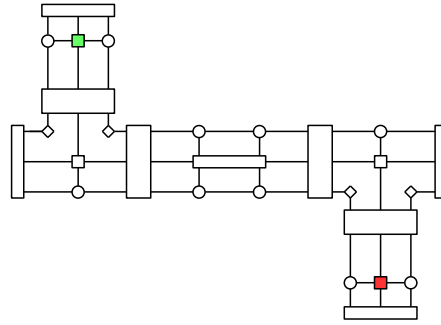
$$\begin{aligned} \langle \Phi_{\vec{\kappa}'}[B'] | \Phi_{\vec{\kappa}}[B] \rangle &= 4\pi^2 \delta^2(\vec{\kappa}' - \vec{\kappa}) \times \left[\text{ [Diagram: A tensor network with a yellow square in the center.] } \right. \\ &+ e^{-i\kappa_V} \text{ [Diagram: A tensor network with a green square at the top and a red square at the bottom.] } + e^{+i\kappa_V} \text{ [Diagram: A tensor network with a red square at the top and a green square at the bottom.] } \\ &+ e^{+i\kappa_H} \text{ [Diagram: A tensor network with a red square on the left and a green square on the right.] } + e^{-i\kappa_H} \text{ [Diagram: A tensor network with a green square on the left and a red square on the right.] } \\ &+ e^{-i\kappa_V} e^{+i\kappa_H} \text{ [Diagram: A tensor network with a green square at the top and a red square on the left.] } + e^{-i\kappa_V} e^{-i\kappa_H} \text{ [Diagram: A tensor network with a green square at the top and a red square on the right.] } \\ &+ e^{+i\kappa_V} e^{+i\kappa_H} \text{ [Diagram: A tensor network with a red square at the bottom and a green square on the left.] } + e^{+i\kappa_V} e^{-i\kappa_H} \text{ [Diagram: A tensor network with a red square at the bottom and a green square on the right.] } \left. \right], \quad (10) \end{aligned}$$

where a green (red) square indicates the transfer operator with a B (B') on the ket (bra) level and the yellow square represents the situation where B and B' are on the same site; the big six-leg tensors represent inverses as in (9), the three-leg tensors are the fixed points of the channels and the diamond tensors are the corner matrices.

The overlap of the Hamiltonian with respect to two excitations can be calculated easily for a frustration-free Hamiltonian: disconnected terms are automatically zero as the Hamiltonian annihilates the ground state locally. The overlap $\langle \Phi_{\vec{\kappa}'}[B'] | \hat{H} | \Phi_{\vec{\kappa}}[B] \rangle$ reduces to a number of local contractions, which we will not write down (as they depend on the form of the Hamiltonian).

Note that the non-frustration free case can be calculated equally well with our methods – provided we have a good

PEPS representation of the ground state. Disconnected terms will generally be of the form



where the middle six-leg tensor represents a two-site Hamiltonian term squeezed between ground state PEPS tensors.